BRAIN–MACHINE INTERFACES

Increasing power efficiency

Narrow-bandwidth signals and relaxed neural-recording parameters can substantially reduce the power requirements of brain–machine interfaces without degrading their performance.

Marc W. Slutzky

Motor brain–machine interfaces (BMIs) detect brain signals, typically from motor cortical areas, and decode intended movements to control an external device[1]. Implanted BMIs have enabled people with tetraplegia to type out words on a computer[2] and to control robotic prosthetic arms[3,4] or their own paralysed limbs via functional electrical stimulation[5]. However, these demonstrations used devices with percutaneous connectors; these limit clinical viability owing to a greater risk of infection, a dependence on caregivers and a lack of cosmetic appeal. Designing completely implantable and wireless BMIs would alleviate these limitations and help translate BMI devices into clinical use. This is possible, yet power-intensive, for current devices that use about 100 microelectrodes to record action potentials (neuronal spikes). For optimal BMI performance, it would be advantageous to increase the number of recording microelectrodes to many thousands. However, this would require significantly more power, which would severely limit battery life. Two independent BMI-design strategies reported in *Nature Biomedical Engineering* now show that power consumption can be reduced with strategies that dispense with the recording of signals at ultrahigh bandwidth (Fig. 1). On one hand, Cynthia Chestek and colleagues show that a high-frequency band (300–1,000 Hz; named the 'spiking-band power' or SBP) with lower power requirements enables closed-loop BMI performance equivalent to the use of spike-detection threshold-crossing events[6] (that is, voltage potentials exceeding the threshold set for each electrode). On the other hand, Nir Even-Chen and colleagues show that the power consumption of BMIs can be reduced by an order of magnitude without loss of performance by relaxing multiple device-design specifications[7].

Chestek and co-authors analysed the SBP and its origins in recordings from Utah microelectrode arrays implanted in the hand area of the motor cortex in non-human primates. They observed that 25–45% of the power of a typical spike waveform is in the SBP range (300–1,000 Hz). This suggests that the SBP contains a substantial proportion of the spikes' bandwidth. By simulating single-neuron activity, they found that the information contained in the SBP may be used to detect signals at lower signal-to-noise ratios than the use of threshold-crossing events. By modelling simulated and actual spike waveforms and firing patterns, the authors examined how spikes from multiple neurons contribute to the SBP. As expected, the SBP reflected mostly the spiking of the nearest units; yet the authors also show that units with higher firing rates contribute more to the SBP than units with low firing rates, and that the firing rate can even

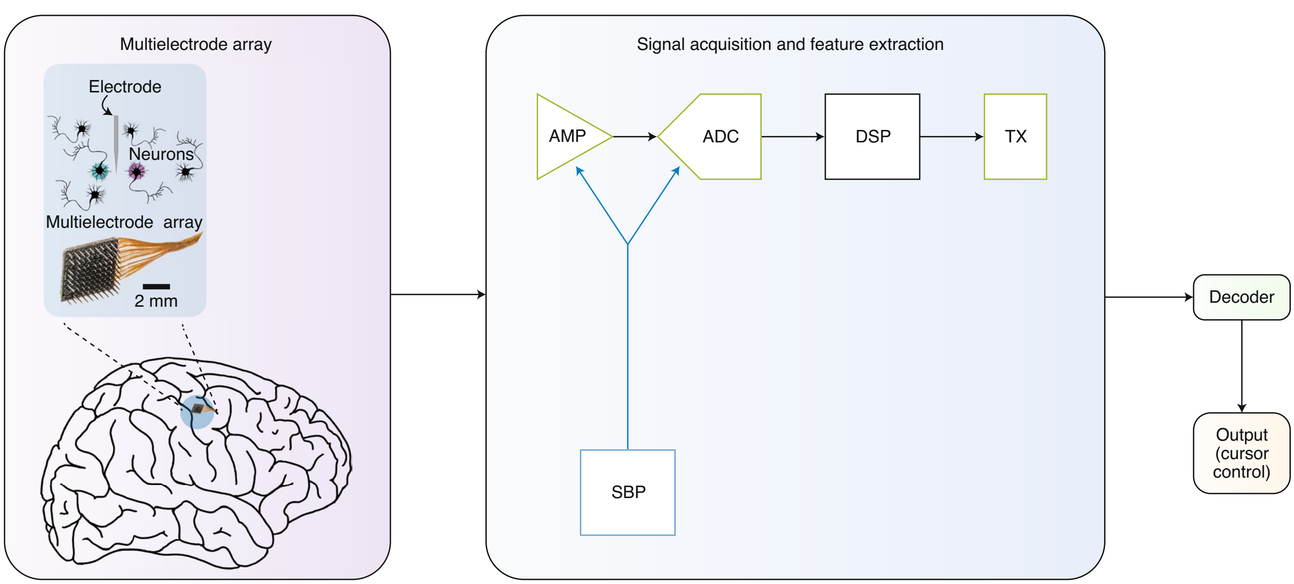

Fig. 1 | Two strategies for reducing the power requirements of brain–machine interfaces. One strategy involves acquiring neural signals from a high-frequency band (the SBP; blue arrows), which reduces the power requirements of the lower-power amplifier (AMP) and the ADC[6]. Another approach involves relaxing signal-quality specifications at the AMP, ADC and wireless transmitter (TX) components (green outlines) of the signal-acquisition and feature-extraction circuit[7]. Neither of these strategies degrade the performance of BMIs. DSP, digital signal processor. Figure adapted with permission from ref. [7], Springer Nature Ltd.

outweigh distance as a determinant of a unit's contribution.

To determine whether the SBP could decode intracortical activity with lower power, Chestek and co-authors examined the ability of the SBP to predict finger kinematics offline and in closed-loop configurations. A similar yet wider spike-band signal (300–6,000 Hz) than that of the SBP had been used to decode offline arm kinematics with high accuracy[8], but not in a closed-loop BMI. In two primates performing finger flexions using separate groups of fingers — either four fingers together or the index finger and fingers 3–5 (with the thumb being finger 1) as two groups of fingers moving simultaneously — the use of the SBP led to similar or better offline decoding performance than the use of threshold crossings. Moreover, the SBP also led to similar or better closed-loop control than threshold crossings in the four-finger-flexion task. Overall, the SBP provided a highly informative signal at a much lower bandwidth (300–1,000 Hz) and at a sampling rate (2 kilosamples per second) that is an order-of-magnitude lower than that required to record threshold crossings (20 kilosamples per second). Because of this, power could be reduced from the 11 mW of current commercially available recording systems to 1.1mW.

Even-Chen and co-authors took a holistic approach to designing BMIs with better power efficiency. The authors first simulated errors in spike detection by randomly changing spikes from detected to undetected (or vice versa) at a given rate (the spike error rate). They found that BMI performances in the offline decoding of data from three monkeys and a paralysed human (from whom pre-recorded data from two-dimensional arm reaches were available) were not significantly affected by spike error rates below 1:1000. This suggests that design constraints in neural interfaces could be relaxed without degrading BMI performance. Neural interfaces are composed of an analogue front end that performs bandpass filtering (to suppress signals of unwanted frequency) and amplification (to enhance the desired neural signals), an analogue-to-digital converter (ADC), a digital signal processor (although not always), and a wireless transmitter (Fig. 1). The authors focused on the effects, on offline decoding performance, of altering bandpass-filter parameters in the analogue front end of a neural interface, in the resolutions of the ADC and in the input-noise floor. They found that bandpass cut-off frequencies could be set to the narrower frequency band of 0.5–3 kHz, that ADCs could sample at 6–7 bits, and that input-noise floors could be raised to 7 μV while maintaining high decoding performance. These relaxed constraints reduced power needs by factors of 20–44 with respect to academic prototype interface systems and conventional systems. Such optimizations could enable fully implantable devices featuring thousands of electrodes.

Furthermore, Even-Chen and colleagues suggest that additional optimizations — circuit-level modifications, such as modifying the analogue processing circuitry and reducing device size, as well as system-level modifications, such as performing dimensionality reduction in hardware and investigating the absolute channel-count requirements for given tasks — may lead to wireless systems with even greater channel capacity. In aggregate, these design modifications could enable the recording of many thousands of neurons or offer longer battery life for the same number of neurons.

The findings of Chestek, Even-Chen and their respective co-authors may enable completely implantable devices with high channel capacities at feasible power requirements. Although many low-power schemes have been proposed (such as the use of on-chip compression[9]), the researchers' optimization techniques are generally simpler and are based on defining the fundamental design requirements specific to BMIs (that is, how the changes affect performance), and their implementation would require relatively minor modifications (few, if any, to the hardware) of existing device designs. Implementing them in combination with on-chip compression schemes should lead to greater power savings.

The use of the SBP circumvents some of the limitations of the use of threshold crossings: the interpretation of multi-unit spikes can limit the neuroscientific questions that can be asked; spike-detection thresholds are often set manually; and systems recording from thousands of neurons may require automated methods to optimize the thresholds and adapt to signal non-stationarities. The use of even lower bandwidth signals (< 300 Hz), such as local field potentials (LFPs), could also reduce power requirements. LFPs tend to carry less information than spikes, but their high-gamma component (70–300 Hz) leads to BMI performances rivalling that of the use of spikes in some cases[2,10]. Two wireless field-potential-based BMI devices (limited to 2 or 4 channels) have been implanted in humans with locked-in syndrome[11,12], and a 64-channel BMI using epidural electrocorticography has been implanted in a person with spinal cord injury[13]. Because LFPs are derived from many thousands of neurons, they have greater longevity and stability than threshold crossings[10,14]. Should SBP-based analysis also prove longer-lasting or more stable than threshold crossings, it would greatly increase the impact of SBP on the clinical viability of BMI devices, given that with current electrode technologies most spikes tend to drop out within approximately five years.

Neural behaviour, during both natural motor tasks and BMI use, is often constrained to low-dimensional manifolds (patterns of coordinated activity across neurons), whose dynamics are highly stable[15]. These manifold-based techniques should be even more relevant to BMI performance when recording from many thousands of neurons. Hence, it will be worth determining whether the optimizations of Chestek and Even-Chen and their colleagues will be equally amenable to manifold-based techniques as traditionally recorded spikes. It will also be important to investigate whether the reduced signal quality imposed by the optimizations can provide advantageous performance improvements (with respect to threshold crossings) in higher dimensional tasks, such as controlling a high-degree-of-freedom prosthetic limb, or in functional electrical stimulation. ❐

Marc W. Slutzky ✉

Departments of Neurology, Physiology, Physical Medicine & Rehabilitation, and Biomedical Engineering, Northwestern University, Chicago, IL, USA.

✉*e-mail: mslutzky@northwestern.edu*

Published online: 22 October 2020
https://doi.org/10.1038/s41551-020-00631-7

References

1. Slutzky, M. W. *Neuroscientist* **25**, 139–154 (2019).
2. Gilja, V. et al. *Nat. Med.* **21**, 1142–1145 (2015).
3. Hochberg, L. R. et al. *Nature* **485**, 372–375 (2012).
4. Collinger, J. L. et al. *Lancet* **381**, 557–564 (2013).
5. Ajiboye, A. B. et al. *Lancet* **389**, 1821–1830 (2017).
6. Nason, S. R. et al. *Nat. Biomed. Eng.* https://doi.org/10.1038/s41551-020-0591-0 (2020).
7. Even-Chen, N. et al. *Nat. Biomed. Eng.* https://doi.org/10.1038/s41551-020-0595-9 (2020).
8. Stark, E. & Abeles, M. *J. Neurosci.* **27**, 8387–8394 (2007).
9. Zhang, J. et al. *IEEE Trans. Circuits Syst. I Regul. Pap.* **63**, 599–608 (2016).
10. Flint, R. D., Lindberg, E. W., Jordan, L. R., Miller, L. E. & Slutzky, M. W. *J. Neural Eng.* **9**, 046006 (2012).
11. Vansteensel, M. J. et al. *N. Engl. J. Med.* **375**, 2060–2066 (2016).
12. Guenther, F. H. et al. *PLoS ONE* **4**, e8218 (2009).
13. Benabid, A. L. et al. *Lancet Neurol.* **18**, 1112–1122 (2019).
14. Flint, R. D., Scheid, M. R., Wright, Z. A., Solla, S. A. & Slutzky, M. W. *J. Neurosci.* **36**, 3623–3632 (2016).
15. Gallego, J. A., Perich, M. G., Chowdhury, R. H., Solla, S. A. & Miller, L. E. *Nat. Neurosci.* **23**, 260–270 (2020).